

82-3-225
高工研圖書室

The Projection Approach to Solenoid Compensation

S. Peggs

Abstract

A general method for analysing solenoid compensation schemes is developed, which projects the effect of each coupling magnet, i.e. a solenoid or a rotated quadrupole, onto a common reference point. This leads to a perturbative method of solution of the exact decoupling conditions.

First order decoupling solutions are demonstrated for local solenoid, local skew quadrupole, and remote solenoid compensation. The merits of five different schemes are compared.

Theoretical and experimental evidence is presented showing how a two skew quadrupole pair scheme can interfere destructively with the beam-beam interaction. The exact compensation of the CLEO solenoid in CESR, using three pairs of skew quadrupoles, is described.

Dispersion coupling is analysed in general. Vertical dispersion is shown to disappear outside any 'straight line' compensation scheme, and a proposal for a vertical emittance knob at CESR is outlined.

1. Introduction

Most storage rings, whether built or planned, incorporate at least one longitudinal magnetic field at the centre of an experimental detector. Uncompensated solenoid fields at the intersection points couple the horizontal and vertical betatron oscillations, dispersions, and emittances. This makes a machine less dynamically stable, and lowers the peak luminosity attainable.

A variety of compensation schemes exist which have been used, or are planned to be used, in order to decouple the equations of motion. The simplest scheme, in use or once used at SPEAR, PEP and CESR, places a half strength anti-solenoid on either side of the experimental solenoid, before the first quadrupole. PETRA reaches satisfactory, but incomplete, compensation by optimum choice of the relative polarities of three experimental solenoids¹. LEP designs^{2,3} and the present CESR mini beta configuration^{4,5,6} compensate with two or three pairs of rotated quadrupoles.

The projection approach⁷ was originally used to design a compensation scheme for the superconducting CLEO solenoid which would place the minimum number of constraints on the intersection region geometry of CESR. Elimination of the proposed superconducting anti-solenoids meant that the first quadrupole Q1 could be moved a lot closer to the intersection point, lowering the vertical beta β_z^* at the IP, and raising the luminosity.

However, projection methods are generally applicable to the quantitative analysis of any weak or intermediate strength coupling system in a lattice. Its simple and powerful perspectives complement the other treatments already available⁸⁻¹³.

2. Coupler Project

The general decoupling problem in a storage ring is represented symbolically in Figure 1. A segment of the lattice, AB, contains the n couplers of interest and a reference point C. Entrance and exit planes of the coupling magnets are labelled 1 through 2n. The insertion as a whole does not couple horizontal (x-x') and vertical (z-z') motion if the four by four transfer matrix across it, T_{BA} , is block diagonal in form.

When all the coupling fields are turned off, the linear motion from any point i to any point j is represented by the block diagonal matrix M_{ij} . Motion across the k'th coupler is given by $N_{2k,2k-1}$. So, the insertion is exactly decoupled if

$$T_{BA} = \left[\begin{array}{c|c} T_{xBA} & 0 \\ \hline 0 & T_{zBA} \end{array} \right] = M_{B,2n} N_{2n,2n-1} M_{2n-1,2n-2} \dots N_{MN} \dots M_{1,A} \quad (1)$$

that is, if eight simultaneous equations containing the n coupler strengths k_1, \dots, k_n are satisfied. It will be shown later that, in the cases of interest, only four of these equations are independent.

This description is simplified if the i'th coupler is represented by its projection matrix, P_i , where

$$P_i = M_{C,2i} N_{2i,2i-1} M_{2i-1,C} \quad (2)$$

because, upon substitution into 1),

$$T_{BA} = M_{BC} (P_n \dots P_2 P_1) M_{CA} \quad (3)$$

so that the exact decoupling conditions become

$$\begin{bmatrix} P_x & 0 \\ \dots & \dots \\ 0 & P_z \end{bmatrix} = P_n \dots P_2 P_1 \quad (4)$$

The projection matrix P_i depends only on the type of coupler represented, on its strength k_i , on the chosen reference point C, and on the state of the intervening non-coupling lattice. It does not depend on the state or location of any other coupler.

This representation is powerful because, in practice, P_i is often very close to the identity matrix, and can be expanded as a polynomial in k_i

$$P_i = I + k_i K_i + k_i^2 \dots \quad (5)$$

Here K_i is a block anti-diagonal matrix. Putting 5) into 4), the general first order decoupling conditions are simply

$$\sum_{i=1}^n k_i K_i = 0 \quad (6)$$

Once the K matrices have been found for couplers in general configurations of interest, 6) is readily solved.

The state of the world outside the insertion really only enters this analysis through the implicit assumption that the rest of the lattice is decoupled. While the K matrices will shortly be conveniently written in terms of Twiss parameters and phases, which are global concepts, in fact they only depend on non-coupling magnet strengths inside the insertion, for a given geometry. In a local insertion the magnet strengths can, in principle, remain fixed during drastic global lattice changes, while in practice they change very little. It should be emphasized here that any local decoupling scheme is essentially independent of the injection/luminosity status of a storage ring, and of the fractional betatron tunes.

2.1 Solenoids

The exact linear matrix, N_s , representing a solenoid of length l , field B , with cylindrically symmetric^s thin fringe fields, can be written as¹⁴

$$N_s = F(l, \theta^2) R(\theta) \quad (7)$$

All the coupling terms are contained in the matrix $R(\theta)$, which represents the rotation of transverse co-ordinates about a longitudinal axis. The angle of rotation, θ , is usually small. For example, using typical values from the CLEO solenoid

$$\theta = \frac{Bl}{2(B\rho)} \approx \frac{1 \times 3}{2 \times 5 \times 3.34} \approx 0.1 \ll 1 \quad (8)$$

$F(l, \theta^2)$ is an uncoupled matrix which only differs from the drift matrix, $L(l)$, by a second order focussing effect, identical in both transverse planes. Since R must commute with the matrix representing any cylindrically symmetric element,

$$[L, R] = [F, R] = 0 \quad (9)$$

But what is the matrix K_s ? If M is the uncoupled matrix from C to the entrance plane of the solenoid, then

$$P_s = I + \theta K_s + \theta^2 \dots = M^{-1} L^{-1} F R M \quad (10)$$

so that, using first order approximations for F and R ,

$$K_s = \begin{bmatrix} 0 & S \\ -S & 0 \end{bmatrix} \quad (11)$$

where

$$S = M_x^{-1} M_z \quad (12)$$

The adjoint (\dagger) transformation of a two by two matrix merely involves reordering the matrix elements

$$\begin{pmatrix} a & b \\ c & d \end{pmatrix} \xleftrightarrow{\dagger} \begin{pmatrix} d & -b \\ -c & a \end{pmatrix} \quad (13)$$

so that, since S has a unit determinant,

$$S^\dagger = S^{-1} = M_z^{-1} M_x \quad (14)$$

An expression will soon be found for K_Q , for skew quadrupoles, which is identical to 11) with S replaced by Q, where Q is a singular matrix.

2.1.1 Solenoids a Drift Away From C

An experimental solenoid centered at C, or an anti-solenoid only a drift away, has the simple K matrix

$$K_s = \begin{bmatrix} 0 & I_2 \\ -I_2 & 0 \end{bmatrix} \quad (15)$$

For a collection of such magnets, as in the simplest compensation scheme, the eight first order decoupling conditions 6) become one condition

$$\Sigma \theta = 0 \quad (16)$$

which is also the exact condition.

2.2 Thin Skew Quadrupoles

A quadrupole, length ℓ and gradient g , which has been rotated about the beam axis by an angle ψ away from midplane symmetry, is represented by the coupling transfer matrix ¹⁴

$$N_Q(\psi, \ell, g) = R(-\psi) N_Q(0, \ell, g) R(\psi) \quad (17)$$

Here $N_Q(0, \ell, g)$ is an uncoupled matrix which does not commute with R .

$$[N_Q, R] \neq 0 \quad (18)$$

Any rotated quadrupole field can be decomposed into a superposition of a regular quadrupole ($\psi = 0$) and a 'skew' quadrupole ($\psi = 45^\circ$). For the present it is convenient to concentrate on thin skew quadrupoles, but later on it will be shown how to deal with thick magnets in a real situation.

A thin skew quadrupole has the coupling matrix

$$N_{45} = \begin{bmatrix} 1 & 0 & | & 0 & 0 \\ 0 & 1 & | & 1/f & 0 \\ \hline 0 & 0 & | & 1 & 0 \\ 1/f & 0 & | & 0 & 1 \end{bmatrix} \quad (19)$$

and has an exact projection matrix

$$P_Q = I + q K_Q = M^{-1} N_{45} M \quad (20)$$

Now, defining the dimensionless strength of a skew quadrupole as

$$q = \frac{(\beta_x \beta_z)^{1/2}}{f} \quad (21)$$

then,

$$K_Q = \begin{bmatrix} 0 & | & q \\ \hline -q^\dagger & | & 0 \end{bmatrix} \quad (22)$$

where, in terms of Twiss parameters at C and at the skew quadrupole

$$Q = \frac{1}{(\beta_x \beta_z)^{\frac{1}{2}}} M_x^{-1} \begin{bmatrix} 0 & 0 \\ 1 & 0 \end{bmatrix} M_z = \begin{bmatrix} -S_x C_z \left(\frac{\beta_x^*}{\beta_z^*} \right)^{\frac{1}{2}} & -S_x S_z (\beta_x^* \beta_z^*)^{\frac{1}{2}} \\ \frac{C_x C_z}{(\beta_x^* \beta_z^*)^{\frac{1}{2}}} & C_x S_z \left(\frac{\beta_z^*}{\beta_x^*} \right)^{\frac{1}{2}} \end{bmatrix} \quad (23)$$

Trigonometric functions of the betatron phases ϕ , with origins at C, are written as

$$S_x = \sin(\phi_x) \quad C_z = \cos(\phi_z) \quad (24)$$

Comparing the expressions for K_s and K_Q , 11) and 22), the first order decoupling conditions 6), for a set of solenoids and skew quadrupoles, have now become the four independent simultaneous equations

$$\sum_i \theta_i S_i + \sum_j q_j Q_j = 0 \quad (25)$$

It appears that, in general, only four couplers are needed to compensate for an experimental solenoid.

3. A First Look at Local Compensation Schemes

Luminosity conditions in an experiment are improved when the intersection region quadrupoles are moved as close as possible to the intersection point. How can compensation be achieved when the immediate anti-solenoids are moved or removed?

3.1 Straight Line Anti-Solenoids

One intuitively promising scheme rotates each thick quadrupole on the east (west) of a solenoid of strength θ by an angle $+\frac{\theta}{2}$ ($-\frac{\theta}{2}$). Anti-solenoids of strength $-\frac{\theta}{2}$ are then placed at convenient locations in the east and the west, decoupling the lattice to all orders of θ .

This conjecture is easily proven, in the absence of bends between the anti-solenoids, if the matrix T_{BA} is written down in terms of its component matrices. When the forms 7) and 17) are used to represent solenoids and rotated quadrupoles, the only coupled matrices present are R matrices. These can all be annihilated by virtue of the commutation relations 9). This procedure does not work in the presence of a bend because R does not commute with the linear dipole matrix.

However, there are practical disadvantages to this compensation scheme. If the experimental field (or energy) is a variable, each individual quadrupole must either rotate mechanically, or, in an approximate scheme, have an attendant skew quadrupole. This becomes unnecessarily complicated if the anti-solenoid is separated from the IP by two or more quadrupoles. Why not just use four skew quadrupoles, and get rid of the anti-solenoids?

Skew quadrupoles have the great advantage of being much shorter than their equivalent solenoids, because a skew field of gradient B/r is β/r times stronger in its coupling effect than a longitudinal field B . This makes them very attractive in the congested lattice geometries near collision points.

3.2 Local Skew Quadrupole Schemes

Compensation of an experimental solenoid is achieved to first order by n thin skew quadrupoles when, according to 15) and 25),

$$\theta \begin{pmatrix} 1 & 0 \\ 0 & 1 \end{pmatrix} + \sum_{i=1}^n q_i Q_i = 0 \quad (26)$$

Most machine lattices are symmetric about an intersection point, so that two points at equal distances on either side of C bear the relationship

$$\beta(-s) = \beta(s) \quad \theta(-s) = -\theta(s) \quad (27)$$

This makes the matrix elements of the general Q matrix, given in 23), even or odd functions of s , according to

$$Q = \begin{pmatrix} \text{odd}(s) & \text{even}(s) \\ \text{even}(s) & \text{odd}(s) \end{pmatrix} \quad (28)$$

Hence two of the decoupling conditions in 26) are automatically satisfied if symmetrically placed skew quadrupole pairs are excited antisymmetrically

$$q(-s) = -q(s) \quad (29)$$

leaving two conditions

$$\theta \begin{pmatrix} 1 & 0 \\ 0 & 1 \end{pmatrix} + 2 \sum_{\substack{i \\ s>0}} q_i \begin{pmatrix} -S_x C_z \left(\frac{\beta_x^*}{\beta_z^*} \right)^{\frac{1}{2}} & 0 \\ 0 & C_x S_z \left(\frac{\beta_z^*}{\beta_x^*} \right)^{\frac{1}{2}} \end{pmatrix} = 0 \quad (30)$$

Only two pairs of skew quadrupoles are necessary to solve these equations. Unfortunately, two skew pair schemes interfere with the beam-beam effect, in a way that straight line anti-solenoid schemes do not. In general it is necessary to use three skew quadrupole pairs. These statements will be expanded shortly, when the subject is rejoined after a discussion of the PETRA compensation scheme.

4. Remote Solenoid Compensation

Consider a storage ring with $2n+1$ experimental solenoids, with n placed on either side of C at identical intersection points, separated in phase from each other by ϑ_x^* and ϑ_z^* . How must the fields of these solenoids be arranged to decouple the motion across them all? This question is important for PETRA where the minimum emittance coupling ratio $\kappa = \frac{\epsilon_z}{\epsilon_x}$, is found empirically by varying the polarities, but not the strengths, of three experimental solenoids.

The S matrix at the i 'th intersection point is given explicitly by

$$S_i = M_x^{-1} M_z = \begin{bmatrix} C_x C_z + S_x S_z \frac{\beta_x^*}{\beta_z^*} & C_x S_z \beta_z^* - C_z S_x \beta_x^* \\ \frac{C_z S_x}{\beta_x^*} - \frac{C_x S_z}{\beta_z^*} & C_x C_z + S_x S_z \frac{\beta_z^*}{\beta_x^*} \end{bmatrix} \quad (31)$$

$$S_x = \sin(i\vartheta_x^*) \quad \text{etc.}$$

After putting this into 25), and using some trigonometrical identities which introduce the sum and difference phases

$$\sigma^* = \phi_x^* + \phi_z^*, \quad \delta^* = \phi_x^* - \phi_z^* \quad (32)$$

the four first order decoupling conditions become

$$\sum_{i=-n}^n \theta_i \begin{pmatrix} \sin & \sigma^* \\ i & \cos \\ & \delta^* \end{pmatrix} = 0 \quad (33)$$

Two of these conditions are automatically satisfied if the solenoid strengths, θ_i , are purely symmetric or antisymmetric. If the solenoid at C is active, the solution cannot be antisymmetric.

Remote solenoid compensation schemes are explicitly sensitive to changes in betatron tune. This means, for example, that explorations of the tune plane at PETRA are restricted by the requirement of satisfactory compensation. Finally, even if a lattice is exactly decoupled, there will always be vertical emittance growth in the major parts of the ring where the one turn matrix is not block diagonal.

5. Skew Quadrupoles and the Beam-Beam Effect

Peak luminosity conditions in electron storage rings are reached by making the vertical collision size of the beams as small as possible, and by colliding the largest currents allowed by the beam-beam interaction. Both of these limits are disrupted, in general, by the skew quadrupoles of a two pair compensation scheme.

When the beam-beam interaction is negligible, at a small current I, the vertical beam size has a contribution due to skew quadrupoles which will be represented by a pseudo-coupling constant χ . That is, for small I,

$$\sigma_z^* = \beta_z^{*\frac{1}{2}} \epsilon_x^{\frac{1}{2}} (\kappa + \chi)^{\frac{1}{2}} \quad \kappa, \chi \ll 1 \quad (34)$$

so even the low current luminosities are reduced. There is a negligible change in the horizontal size.

At high currents the situation gets even worse, because the beam-beam equations of motion are destructively modified by the presence of skew quadrupoles. There is more beam-beam blow-up, and the maximum stable current is reduced.

These problems would all disappear if the one turn matrix at C itself was block diagonalised, that is if the sets of couplers on the west and east of C were independently balanced. This would require four pairs of skew quadrupoles. In fact three pairs are sufficient to free the collision performance of a storage ring from the compensation scheme.

These comments will now be justified, at first theoretically, and then experimentally.

5.1 Theory

A useful 'normalised' system of coordinates (capitals) at the crossing point is related to the 'physical' system (lower case) by

$$\begin{aligned} X &= \frac{x}{(\beta_x^* \epsilon_x)^{1/2}} & Z &= \frac{z}{\kappa^{1/2} (\beta_z^* \epsilon_z)^{1/2}} \\ X' &= x' \left(\frac{\beta_x^*}{\epsilon_x} \right)^{1/2} & Z' &= \frac{z'}{\kappa^{1/2}} \left(\frac{\beta_z^*}{\epsilon_z} \right)^{1/2} \end{aligned} \quad (35)$$

In the flat beam limit, $\kappa \ll 1$, a statistically typical unperturbed particle rotates around unit radius circles in horizontal and vertical normalised phase space planes. It advances by an angle $2\pi Q$ between each crossing.

The beam-beam impulse is also conceptually simple in the normalised system, namely

$$\Delta X' = -4\pi \xi_x X g(X) \quad \Delta Z' = -4\pi \xi_z Z f(X, Z) \quad (36)$$

Here f and g are positive form factors, even functions of X and Z , which drop below one for finite amplitude particles. Beam-beam instability in either plane occurs, very roughly speaking, when $4\pi \xi$ is comparable to 1, because then the angular kick a typical particle receives is comparable to its amplitude.

When a balanced set of couplers is turned on, a particular trajectory coming into the insertion will be distorted, acquiring new coordinates at the IP which will be denoted by a subscript C (e.g. X_C, x_C). The old coordinates are still useful, however, because they label the exterior trajectories, which the compensation scheme does not disturb. The true stability of a trajectory is determined by writing the coupled beam-beam impulse in terms of uncoupled natural coordinates.

The linear relationship between coupled and uncoupled physical coordinates, for a decoupling scheme with n-1 pairs of skew quadrupoles, is simply

$$\begin{bmatrix} x_c \\ x'_c \\ z_c \\ z'_c \end{bmatrix} = P_W \begin{bmatrix} x \\ x' \\ z \\ z' \end{bmatrix} \quad P_W = P_{-1} P_{-2} \dots P_{-n} \quad (37)$$

This is illustrated in figure 2. It is conceptually convenient, here, to break the experimental solenoid into two halves, with equal and opposite fringe fields an infinitesimal distance on either side of the collision point. This does not affect any of the physical conclusions of this discussion.

If motion across the whole insert has been properly decoupled, then P_W is generally parameterized, to first order, by

$$P_W = \begin{bmatrix} 1 & 0 & 0 & \chi^{1/2} (\beta_x \beta_z)^{1/2} \\ 0 & 1 & b & 0 \\ 0 & \chi^{1/2} (\beta_x \beta_z)^{1/2} & 1 & 0 \\ b & 0 & 0 & 1 \end{bmatrix} \quad (38)$$

where χ is the pseudo coupling constant introduced in 34), and where

$$\chi^{1/2} = \sum_{WEST} q \sin(\phi_x) \sin(\phi_z) \quad (39)$$

Since the matrix elements P_{W13} and P_{W31} are identically zero, the beam ribbon at the IP in a successful compensation scheme is not tilted.

The matrix elements b essentially measure the screw pitch of the beam ribbon. Because b does not affect the size of the beam, and does not appear below in the modified beam-beam equations, it may be ignored. A fourth skew quadrupole pair is not necessary.

In the case of interest the effect of the skew quads is strong, but the beams remain flat. That is,

$$\chi^{1/2} \ll |\chi|^{1/2} \ll 1 \quad (40)$$

so that the coupled and uncoupled natural displacements are related by

$$X_c = X \quad Z_c = \left(\frac{\chi}{\kappa}\right)^{1/2} X' \quad (41)$$

The beams are blown up vertically but not affected horizontally, so the beam-beam impulse, in a mixture of coupled and uncoupled coordinates, becomes

$$\Delta X'_c = -4\pi\xi_x Xg(X) \quad \Delta Z'_c \approx 0 \quad (42)$$

In consistent natural uncoupled coordinates, the beam-beam impulse becomes

$$\begin{aligned} \Delta X' &= -4\pi\xi_x Xg(X) & \Delta Z' &\approx 0 \\ \Delta X &= 0 & \Delta Z &= \left(\frac{\chi}{\kappa}\right)^{1/2} 4\pi\xi_x Xg(X) \end{aligned} \quad (43)$$

When such a coupling scheme is turned on, the exterior world sees no change in the horizontal motion of a typical particle, but sees enormous vertical beam-beam kicks, which are apparent displacements.

Skew quadrupoles interfere dangerously with the beam-beam effect, unless care is taken to ensure that χ is much smaller than κ . Ideally,

$$\chi^{1/2} = \sum_{s > 0} -q \sin(\phi_x) \sin(\phi_z) = 0 \quad (44)$$

5.2. Experimental Results at CESR

A local two skew pair compensation scheme was tested at CESR in April 1981, with a constant field of 0.4 Tesla in the CLEO solenoid.¹⁵ Observations were made with the skew strengths at various fractions of their theoretical decoupling solution. Their strengths were conveniently parameterized by $\chi^{1/2}$, which was 0.18 for full compensation, a value comparable or larger than $\kappa^{1/2}$.

Single beam measurements of the vertical dispersion η_z around CESR gave quantitative confirmation that the theoretical decoupling strengths were correct. Coupled vertical dispersion waves outside a straight line compensation scheme in a lattice with finite η_z^* only disappear when the insertion is properly decoupled.

Colliding beam measurements of the specific luminosity $\frac{L}{I^2}$ as a function of skew strength $\chi^{1/2}$ are shown in figure 3, as they were taken for three different beam currents.

In the low current case, $I = 2.7$ mA, the beam-beam interaction was negligible, and the specific luminosity depended on χ and κ through the vertical size σ_z^* as given in 34). When the skew quadrupoles were off, $\chi^{1/2} = 0$, the substantial lattice coupling made both $\kappa^{1/2}$ and σ_z^* large. Near the decoupled setting, $\chi^{1/2} = 0.18$, $\kappa^{1/2}$ was a minimum, but $\chi^{1/2}$ was large enough to dominate the vertical size.

At the intermediate current, $I = 5.4$ mA, the average specific luminosity was less and the optimum skew strength decreased, lowering the curve and moving it leftward. The beam-beam effect was being felt, and was having most effect at large $\chi^{1/2}$ values, in qualitative agreement with theory.

With currents approaching the usual beam-beam limit in CESR, $I = 12.0$ mA, it was impossible to turn the skew quadrupoles up to more than half their decoupling strengths.

5.3 Conclusions

If an experimental solenoid is strong enough to need compensation, that is, if

$$\chi^{1/2} \sim q \sim \theta \geq \kappa^{1/2} \quad (45)$$

then a two skew quadrupole pair scheme will only be satisfactory if judicious phase locations are available, and can be maintained. In the present LEP scheme, with skew quads five and seven regular quads away from an IP, there is not enough phase stability to compensate in both 60° and 90° lattices. An experimental solenoid usually needs three pairs of skew quadrupoles for successful compensation.

6. Compensation at CESR with Three Skew Quadrupole Pairs

In September 1981 CESR resumed operation with a mini-beta geometry at both crossing points, and with a 1.5 Tesla superconducting solenoid in the CLEO experiment. Figure 4 shows the crowded geometry of the lattice elements between the south IP and the first soft dipole. Quadrupole Q1 is mounted on rails and slides back along the vacuum chamber, allowing rapid experimental access, but denying the only possible location for a local anti-solenoid.

Projection techniques were incorporated in a computer program, SKEW, to design the three skew pair compensation scheme which best fits the practical constraints^{5,6}. Now used regularly in an operational mode, SKEW determines the exact decoupling strengths of real couplers in a given lattice, and calculates, for example, the second order tune shifts and the dispersion perturbations.

6.1 Finding the Exact Decoupling Solution with SKEW

On a first pass SKEW assumes that all skew quadrupoles are thin, and finds a decoupling solution only to first order in θ . Then, however, it calculates an error vector \bar{p} using exact transfer matrices for the solenoid and for the thick skew quadrupoles, and approaches the exact solution iteratively. Two or three iterations are usually sufficient to reduce the apparent residual field in CLEO to less than one gauss.

The components of the error vector

$$\bar{p} = \begin{pmatrix} p_1 \\ p_2 \\ p_3 \end{pmatrix} \quad (46)$$

are just the coupling matrix elements of the exact projection matrix P_E which must be reduced to zero.

$$P_E = \left[\begin{array}{cc|cc} & & p_1 & p_3 \\ & P_X & b & p_2 \\ \hline -p_2 & p_3 & & \\ b & -p_1 & P_Z & \end{array} \right] \quad (47)$$

Here P_X and P_Z differ from unit matrices by second order (θ^2) terms which represent, for example, the focussing effect of the solenoid.

Two more vectors are necessary for a compact iterative algorithm. The implicitly antisymmetrical excitation of the skew quads is written as

$$\bar{q} = \begin{pmatrix} q_1 \\ q_2 \\ q_3 \end{pmatrix} \quad (48)$$

while the location of the i 'th skew quadrupole is described by the vector

$$\bar{a}_i = \left[\begin{array}{c} -S_x C_z \left(\frac{\beta_x^*}{\beta_z^*} \right)^{\frac{1}{2}} \\ C_x S_z \left(\frac{\beta_z^*}{\beta_x^*} \right)^{\frac{1}{2}} \\ -S_x S_z (\beta_x^* \beta_z^*)^{\frac{1}{2}} \end{array} \right]_i \quad (49)$$

Now, defining the influence matrix A as

$$A = \left[\bar{a}_1, \bar{a}_2, \bar{a}_3, \right] \quad (50)$$

then, using 15), 23) and 39), the error vector to first order and with thin lenses is

$$\bar{p} = A\bar{q} + \frac{\Theta}{2} \begin{bmatrix} 1 \\ 1 \\ 0 \end{bmatrix} \quad (51)$$

so that the first order decoupling solution is just

$$\bar{q} = -\frac{\Theta}{2} A^{-1} \begin{bmatrix} 1 \\ 1 \\ 0 \end{bmatrix} \quad (52)$$

Iteration is straightforward with this notation. If \bar{p} is calculated exactly using an old set of excitations \bar{q}_{old} , a better set will be

$$\bar{q}_{new} = \bar{q}_{old} - A^{-1} \bar{p}_{old} \quad (53)$$

6.2 Skew Quadrupoles Locations

Soon it will be shown that only skew quadrupoles beyond the first soft bend, B1, couple horizontal dispersion into vertical dispersion. Unfortunately for CESR the vector \bar{a} is almost constant between Q1 and B1, leading to unreasonably large excitations unless one skew quad is outside B1. The strength of the third skew quad and its dispersion coupling effect are minimised by choosing a location where the length of \bar{a}_3 is maximised.

Since the vector \bar{a}_3 is dominated in length and direction by its first component so that

$$|\bar{a}_3| \approx \left(\frac{\beta_x^*}{\beta_z^*} \right)^{\frac{1}{2}} |\sin(\phi_{x3}) \cos(\phi_{z3})| \quad (54)$$

and an ideal location has phases

$$\phi_{x3} = \left(m + \frac{1}{2}\right)\pi \quad \phi_{z3} = n\pi \quad (55)$$

where m and n are integers.

Because the first two skew quadrupoles are so close to the IP₁ and because the direction of a₃ is quite fixed, the solution vectors q₁, a₁ and q₂, a₂ are almost totally independent of global lattice parameters. This preserves the high level of lattice flexibility that is one of CESR's virtues. However, the two vectors cannot be well orthogonalised, and comparatively large integrated skew gradients of around 1.0 Tesla are necessary. These fields are produced by mechanical rotation of Q1 and Q2, through independent angles of up to ± 0.1 radians. At a typical energy of 5.0 GeV the angles are close to (but not equal to) $\frac{\theta_{CLEO}}{2}$, about 0.05 radians at a solenoid field of 1.0 Tesla.

The third skew quadrupole, placed just outside Q11 about 70 metres from the IP, is comparatively weak, typically about 0.1 Tesla. Built as a current sheet magnet, 0.26 metres long, it can be simultaneously used as a steering magnet. Its location is not only advantageous because of the phase conditions (55), but also because the dispersion coupling, which will now be analysed in general, is very weak there.

7. Chromatic Effects

So far, by using a four by four linear matrix analysis, it has been implicitly assumed that all particles have the nominal design energy. A better approximation labels each particle with a constant relative energy error, $\delta = \frac{\Delta E}{E}$, and defines the dispersion function, η , by saying that the equilibrium orbit of a particle is displaced by $\eta_x \delta$ and $\eta_z \delta$.

The conventional solenoid-antisolenoid compensation scheme is unique in decoupling particles of all energies. In general, however, a compensated insertion will cause off energy particles to perform coupled betatron oscillations about their new equilibrium orbits. Small oscillations can still be described in a four by four matrix formalism by a linearisation scheme⁷ if the second order transfer matrices are known.

Comparisons of compensation schemes on the basis of their 'coupling chromaticity' could be made in this way, but the process would be quite tedious, and the results would depend on the distribution of sextupoles. In practice it is enough to study the analytic behaviour of off energy particles without betatron oscillations.

What is the vertical dispersion function η_z , around a machine with a given compensation scheme? How should couplers be placed to minimise η_z and the vertical emittance?

7.1 Dispersion Coupling

The differential equations for coupled dispersions

$$\eta_x'' - K\eta_x = Q\eta_z + B\eta_z' + G_x \quad (56)$$

$$\eta_z'' + K\eta_z = Q\eta_x - B\eta_x'$$

are identical to those for coupled betatron oscillations

$$\begin{aligned} x'' - Kx &= Qz + Bz' \\ z'' + Kz &= Qx - Bx' \end{aligned} \quad (57)$$

except for the horizontal dipole term, $G_x = \frac{1}{\beta_x}$, which drives the dispersion 'oscillations' around the lattice. In these equations B stands for solenoid fields, and Q stands either for skew quadrupole fields or for cylindrically symmetric solenoid fringe fields.

If B and Q are even and odd functions about an IP, as in most compensation schemes, then, applying periodic boundary conditions to 56), η_x and η_z are respectively even and odd. In a machine with only two crossing points, like CESR, the important beam-beam condition

$$\eta_z^* = 0 \quad (58)$$

is automatically satisfied at both experiments.

The vertical dispersion solution of 56) is found by breaking up the horizontal dispersion into a local part, η_o , and a global part, η_b , so that

$$\eta_x = \eta_o + \eta_b \quad (59)$$

The local part is chosen to be zero at the IP, and is propagated through the insertion region as if all the couplers were turned off. That is,

$$\eta_o^* = 0 \quad \eta_o' - K\eta_o = G_x \quad (60)$$

Now, using 59) and 60), and taking $B\eta_o'$ to be zero, 56) becomes

$$\begin{aligned} \eta_b' - K\eta_b &= Q\eta_z + B\eta_z' \\ \eta_z' + K\eta_z &= Q\eta_b - B\eta_b' + Q\eta_o \end{aligned} \quad (61)$$

These equations are analogous to coupled betatron oscillations 57), with vertical dipole steering fields $Q\eta_o$. Assuming that the lattice is decoupled, the vertical dispersion at a general point outside the insertion is then just

$$\frac{\eta_z}{\beta_z^{1/2}} = \frac{\sin(\phi_z - \pi Q_z)}{\sin(\pi Q_z)} \sum_i q_i \frac{\eta_{oi}}{\beta_{xi}^{1/2}} \sin(\phi_{zi}) \quad (62)$$

where the sum is taken over only one member of each antisymmetrically powered skew quadrupole pair.

Straight line compensation schemes of any kind do not disturb the vertical dispersion outside the insertion, because η_{0y} is identically zero up to the first horizontal dipole. Such schemes do not introduce any vertical emittance.

There is always vertical emittance growth at the bends inside the CLEO insertion, due to the non zero vertical dispersion and to the twisting of the trajectories. However, the main contribution, due to vertical dispersion outside the insertion, is minimised by choosing a location for the third skew quad where all three terms in the sum in (62) are small.

Despite lattice variations of η_{x3} and η_{x3} , the local dispersion η_{0y} at Q11 is consistently less than 0.1 metres in magnitude, much less than the peak η_{0y} values of about 3 metres. Typical vertical dispersion waves then have amplitudes of about 0.02 metres, which is near the limit of experimental resolution. PETROS¹⁶ simulations in a range of CESR lattices predict emittance coupling values, K , of between 3×10^{-4} and 7×10^{-4} .

7.2 A Vertical Emittance Knob

Finally, it is natural in the context of dispersion coupling to describe a scheme, proposed at CESR, which puts a controlled amount of vertical emittance into the beams.¹⁷ Remote skew quadrupoles, at Q14 and Q29, are excited and balanced to produce vertical dispersion round the ring without disturbing any colliding beam parameters except the vertical emittance.

It is quite straightforward in practice to impose the two phase advance constraints on CESR lattices

$$\phi_{x29} - \phi_{x14} = i \pi \qquad \phi_{z29} - \phi_{z14} = j \pi \qquad (63)$$

where i and j are integers. Now, if the two (thin) skew quadrupoles in the east are excited such that

$$q_{14} + (-1)^{i+j} q_{29} = 0 \qquad (64)$$

then their total projection matrix is identically the unit matrix.

$$\begin{aligned} P_E &= (I + q_{29} K_{Q29})(I + q_{14} K_{Q14}) \\ &= (I - q_{14} K_{Q14})(I + q_{14} K_{Q14}) \equiv I \end{aligned} \qquad (65)$$

Not only are the betatron oscillations at the crossing points exactly decoupled, but also there is a total absence of higher order perturbations like second order tune shifts.

It is necessary to power the east and west skew quadrupoles antisymmetrically, not to decouple the whole insertion, but rather to make η^* identically zero. If i is an even number, then according to 56) or 62) the vertical dispersion waves will be roughly confined between Q14 and Q29. It is more convenient for the manufacture of vertical emittance if i is odd, because then vertical dispersion is made all round the ring.

If skew quadrupoles of strength $|q|$ couple peak horizontal dispersions $\hat{\eta}_x$ into a vertical dispersion wave of amplitude $\hat{\eta}_z$ around the lattice, then a very crude estimate of the coupling constant created is

$$\kappa^{\frac{1}{2}} \approx \frac{\hat{\eta}_z}{\hat{\eta}_x} = |q| \quad (66)$$

Since a regular quadrupole in a normal cell has a $|q|$ value very close to 2, even comparatively weak skew quadrupoles are strong enough to produce a useful amount of vertical emittance.

Acknowledgements

I would like to thank the CESR machine group for their support. Assistance and advice came particularly from Ken Adams, Raphael Littauer, Stu Peck and Dick Talman.

References

1. Piwinski et al., DESY M-80/03 (1980).
2. G. Guignard, LEP-70/75 (1978).
3. G. Guignard, LEP Note 199 (1979).
4. K. Adams, CESR Note CBN-81-5 (1981).
5. S. Peggs, CESR Note CBN-81-17 (1981).
6. S. Peggs, CESR Note CBN-81-24 (1981).
7. S. Peggs, Ph.D. Thesis, Cornell University (1981).
8. P. Bryant, CERN ISR-MA/75-28 (1975).
9. A. Chao and M. Lee, J. Appl. Phys. 47, 4453 (1976).
10. G. Guignard, CERN 76-06 (1976).
11. G. Guignard, CERN 78-11 (1978).
12. P. Bryant, CERN ISR-BOM/79-16 (1979).
13. M. Bassetti, CERN ISR-TH/79-41 (1979).
14. K. Brown et al., CERN 73-16 (1973).
15. CESR Log 37, 139 (1981).
16. J. Kewisch, Diplomarbeit, DESY (1978).
17. S. Peggs, CESR Note CBN 81-26 (1981).



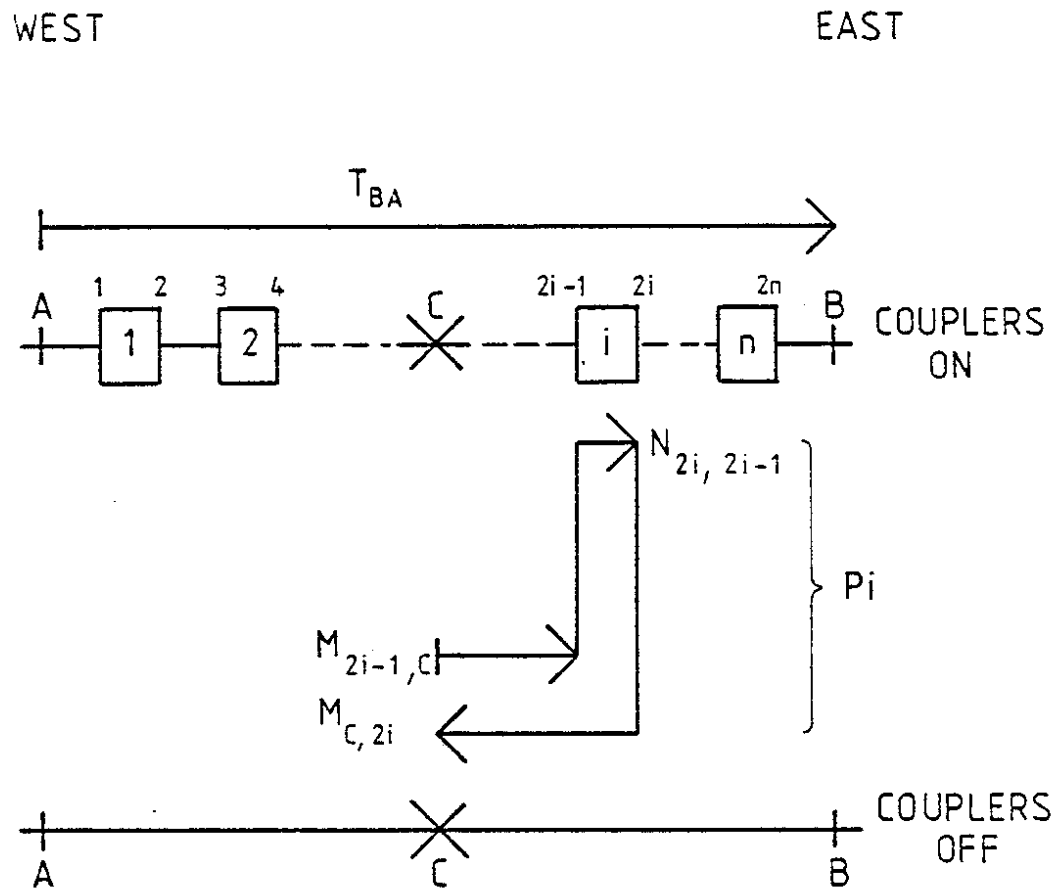


Fig. 1 Symbolic description of couplers and transfer matrices near a reference point C in an insert AB

WEST

EAST

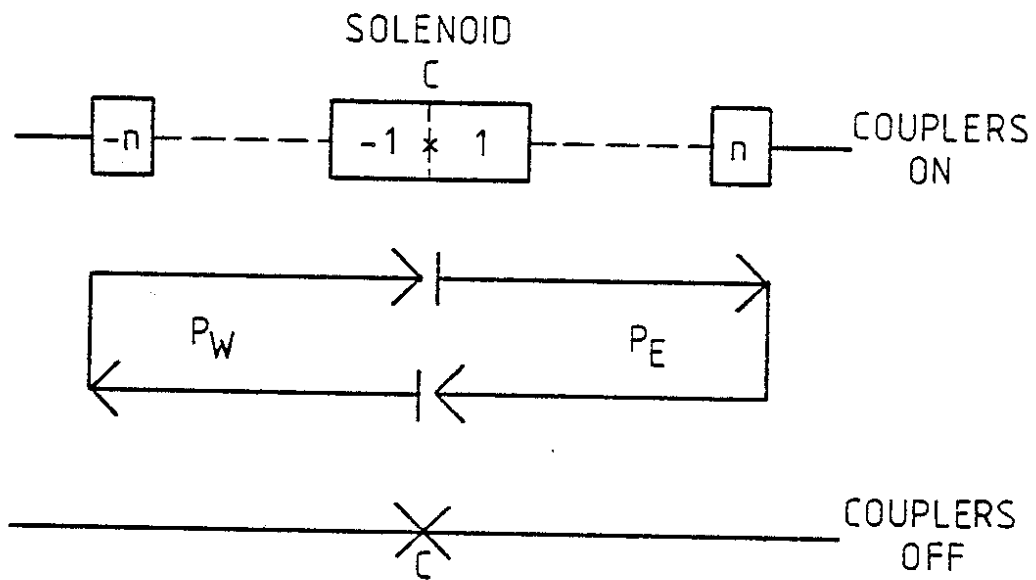


Fig. 2 The west and east projection matrices P_W and P_E .

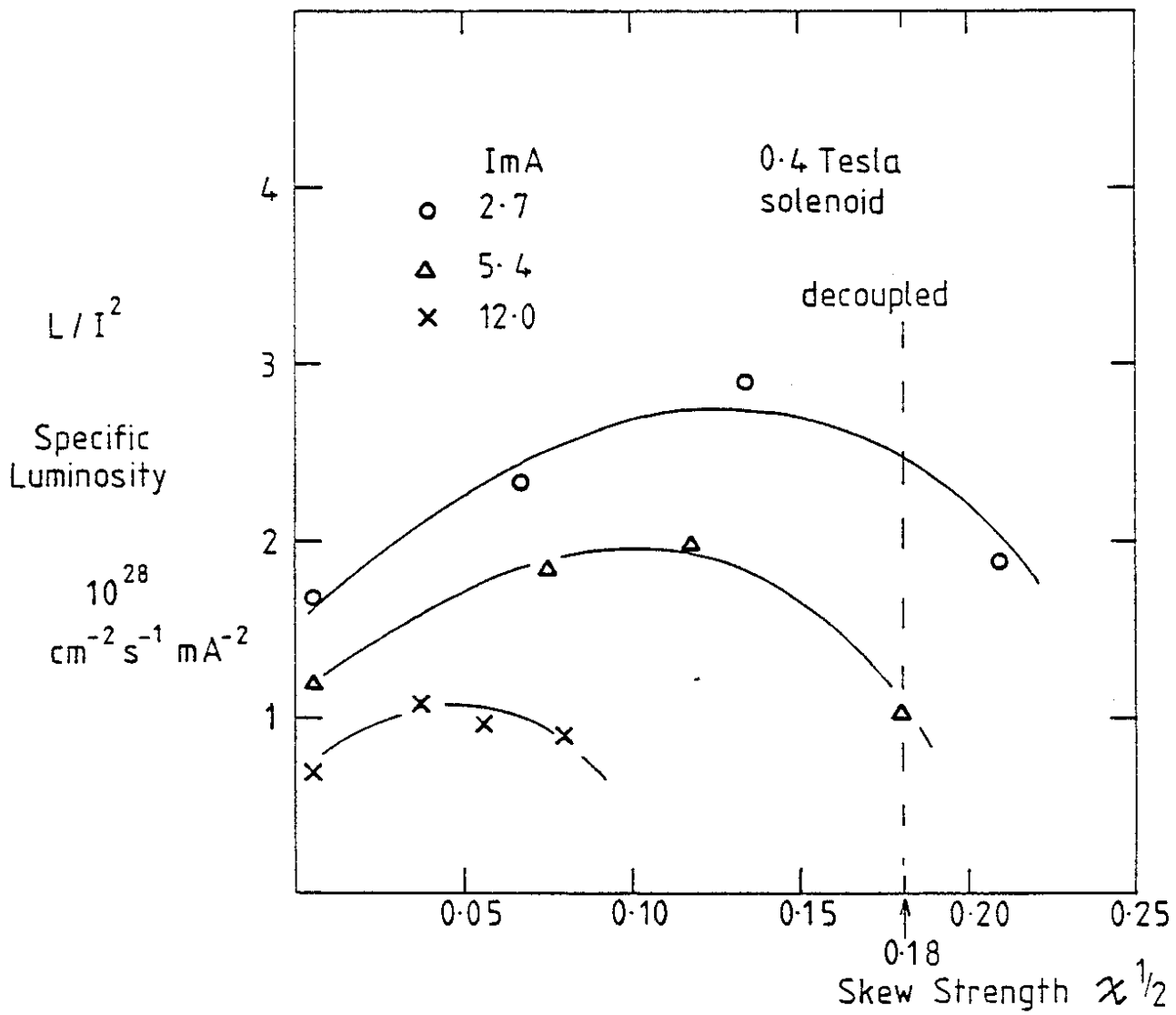


Fig. 3 Specific Luminosity versus Skew Strength in a trial two skew quadrupole pair compensation scheme in CESR.

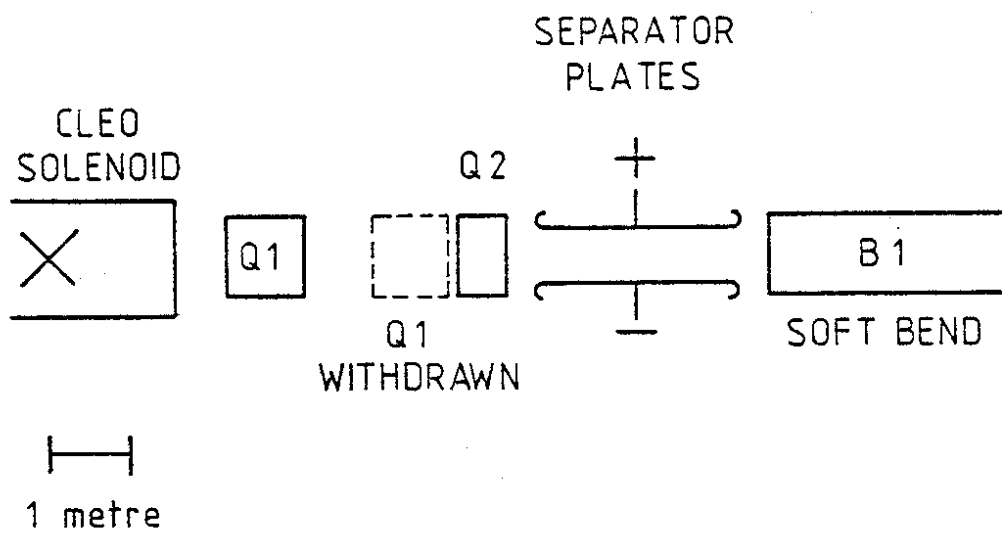


Fig. 4 The CESR mini-beta geometry just east of CLEO.